Letter

Superconducting pairing symmetry in $MoTe_2$

M. M. Piva,[1,*] L. O. Kutelak,[1,2] R. Borth,[1] Y. Liu,[3,†] C. Petrovic,[3] R. D. dos Reis,[2] and M. Nicklas[1,‡]

[1]*Max Planck Institute for Chemical Physics of Solids, Nöthnitzer Straße 40, D-01187 Dresden, Germany*

[2]*Brazilian Synchrotron Light Laboratory (LNLS), Brazilian Center for Research in Energy and Materials (CNPEM), Campinas, 13083-970 Sao Paulo, Brazil*

[3]*Condensed Matter Physics and Materials Science Department, Brookhaven National Laboratory, Upton, New York 11973, USA*

(Received 25 April 2023; accepted 31 October 2023; published 16 November 2023)

Topological superconductors have long been sought for their potential use in quantum computing. The type-II Weyl semimetal $MoTe_2$ is an obvious candidate, exhibiting a superconducting state below 500 mK at ambient pressure, but the question remains whether the pairing is conventional s^{++} or topological s^{+-}. The application of external pressure favors the superconducting state in $MoTe_2$ and suppresses the structural transition from $1T'$ to T_d. The competition between the two structures leads to a mixed phase that strongly enhances the disorder present in the system, remarkably without affecting the superconducting transition temperature, in contrast to the expectation of s^{+-} pairing superconductivity. Our thorough analysis of the electrical and Hall resistivities as a function of pressure yields the most accurate temperature-pressure phase diagram available to date for $MoTe_2$ and a detailed view of the relationship between disorder and superconductivity, supporting a conventional s^{++} pairing symmetry.

DOI: 10.1103/PhysRevMaterials.7.L111801

Much effort is devoted to the search for new materials that will enable the development of more efficient computing and storage systems [1]. In this regard, compounds or devices hosting Majorana fermions are being extensively sought. These particles are their own antiparticles, obey non-Abelian statistics, and have the potential to be used in fault-tolerant quantum computing [1–4].

Topological superconductors are promising materials to host Majorana fermions or Majorana zero modes. They exhibit gapless excitations in their nontrivial surface states and an electron-pair condensate, which is a charge neutral ground state where electrons and holes are indistinguishable, allowing them to be their own antiparticles [2,5]. Topological superconductivity was predicted to be realized in fully gapped superconductors with odd parity symmetry, such as p-wave superconductors [6], where Majorana fermions could exist in the vortex cores of these materials [2]. Recently it has been found that topological superconductivity is also possible in s-wave superconductors [7]. For example, in time-reversal invariant Weyl semimetals with s^{+-} superconductivity, a topological superconducting state might be present when the sign change of the superconducting gap occurs between Fermi surfaces of opposite Chern numbers [8].

The transition metal dichalcogenides are excellent candidates to host topological superconductivity. These materials have the chemical formula TX_2 (T = transition metal, X = chalcogenide) and many are predicted to be Dirac or Weyl semimetals [2]. Of particular interest is $MoTe_2$ [9], which has three different structural phases [10]. A hexagonal $P6_3/mmc$ structure ($2H$ phase) is observed in semiconducting samples, but this phase can be easily tuned to the monoclinic $P2_1/m$ structure ($1T'$ phase), due to the low energy barrier between these structures. Finally, $MoTe_2$ can also exhibit a noncentrosymmetric orthorhombic $Pmn2_1$ structure (T_d phase), which is stable at low temperatures or in thin films [11–13]. At ambient pressure, a first-order structural transition is observed at $T_s \approx 250$ K from the high-temperature $1T'$ phase to the T_d phase [9,10,14–22]. The variety of structural phases present in $MoTe_2$ and the small energy scales required to tune them suggest that structural disorder may play an important role in this material and that polymorphs might be kinetically stabilized, as is common in chalcogenides [23].

In the T_d phase, $MoTe_2$ is a type-II time-reversal invariant Weyl semimetal superconductor with a transition temperature (T_c) around 500 mK at ambient pressure [24,25]. The presence of both nontrivial topology and superconductivity has led to extensive studies investigating the possibility of topological superconductivity in $MoTe_2$ [26], however the superconducting pairing symmetry is still unknown. Muon spin rotation (μSR) [27], point contact spectroscopy [28], and electronic gating experiments [29] revealed two-band superconductivity, suggesting unconventional s^{+-} or conventional s^{++} pairing mechanisms, as observed in most of the iron pnictides [30] and MgB_2 [31]. A strong argument in favor of the s^{+-} pairing is the suppression of T_c with increasing disorder, as observed

*Mario.Piva@cpfs.mpg.de

†Present address: Los Alamos National Laboratory, Los Alamos, New Mexico 87545, USA.

‡Michael.Nicklas@cpfs.mpg.de

in $MoTe_2$ samples with different residual resistance ratios (RRRs) [25]. However, this cannot explain the enhanced T_c observed in sulfur or Ta-doped samples [32–34]. Also μSR experiments cannot discriminate between s^{+-} and s^{++}. Furthermore, other transport measurements have not detected a superconducting state down to 25 mK in high quality single crystals [15], while others claim that superconductivity resides in the $1T'$ phase [35]. Therefore, the realization of a superconducting nontrivial s^{+-} phase in T_d $MoTe_2$ is strongly debated.

The application of external pressure suppresses the structural transition and strongly enhances T_c, as previously observed in many reports [15–19,27]. However, a gray area remains in the temperature-pressure (T-p) phase diagram of $MoTe_2$, the so-called mixed-phase region, where both T_d and $1T'$ structural phases are present. The existence of these different structural domains increases the disorder in the material, leading to higher residual resistivities and suppressed quantum oscillation amplitudes [18,19]. This enhancement of disorder may allow us to distinguish between s^{+-} and s^{++} superconductivity in $MoTe_2$, as was previously demonstrated for iron pnictides [36].

In this Letter we report a detailed study of the T-p phase diagram of $MoTe_2$ using longitudinal and Hall resistivity measurements. Our data, taken at very small pressure steps, provide the most accurate T-p phase diagram available to date for $MoTe_2$ and a detailed view of the relationship between structural phase transitions and superconductivity. A strong enhancement of the structural disorder in the mixed-phase region was observed, remarkably without affecting the superconducting state, in contrast to the expectation for a s^{+-} pairing state. Our findings shed light on the pairing symmetry of the low-pressure superconducting state of $MoTe_2$ and favor a conventional s^{++} pairing mechanism.

The electrical transport properties of single crystalline $MoTe_2$ grown from Te flux [22,24] were studied under hydrostatic pressure using a piston-cylinder-type pressure cell with silicon oil as the pressure transmitting medium and lead as the pressure gauge [37]. The magnetic field was applied parallel to the c axis and the current was perpendicular to the field. Temperatures down to 50 mK and magnetic fields up to 9 T were achieved in different commercial cryostats.

The T-p phase diagram of $MoTe_2$ has been reported in several works before [15–21,27,35,38], and for bulk samples a consensus has been reached.

(i) At ambient pressure, a first-order-type structural transition from the $1T'$ to the T_d phase takes place around 250 K, which is suppressed to zero temperature in the vicinity of 1 GPa.

(ii) At low temperatures, a superconducting phase is present in the entire temperature-pressure phase diagram up to 3 GPa and beyond.

Only the early work of Qi *et al.* [16] reported the presence of a structural transition up to about 3 GPa, which was not confirmed by later studies. This work has also led to the misconception that there is an almost instantaneous increase in T_c within the T_d phase below 1 GPa. All of the more recent studies show a smooth increase in T_c [17,18,20,27,35].

The behavior summarized above is also observed in our Letter. We find an anomaly in the temperature dependence of

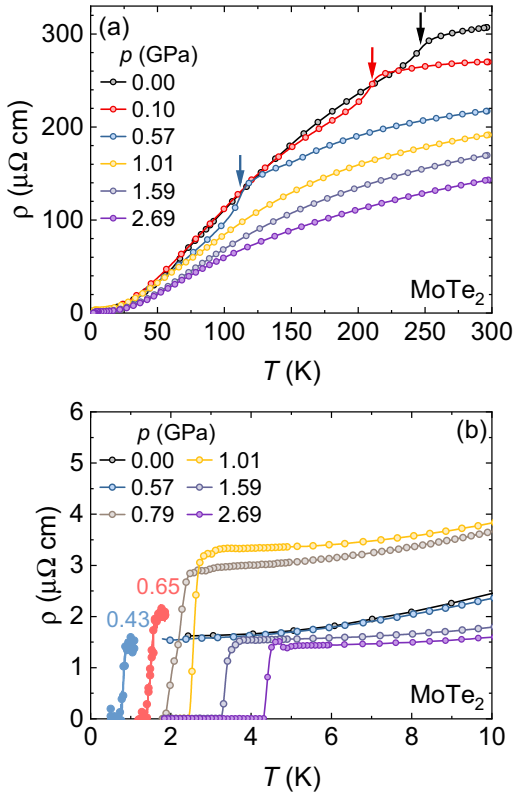

FIG. 1. (a) Electrical resistivity (ρ) as a function of temperature for selected pressures. The arrows indicate the structural transition temperature. (b) Enlarged view of the low-temperature region.

the electrical resistivity $\rho(T)$ that characterizes the first-order structural transition from $1T'$ to T_d at 246(2) K at ambient pressure [see the black arrow in Fig. 1(a)]. Increasing pressure suppresses the structural transition temperature T_s to 53(5) K at 0.87 GPa. Above this pressure, our $\rho(T)$ data show no evidence for the structural phase transition. Already at 0.93 GPa any feature is missing.

To further investigate the first-order-like suppression of T_s, we performed temperature runs at closely spaced pressure points in the region around the critical pressure $p_c \approx 0.9$ GPa. These data confirm the sudden suppression of T_s and show a remarkable change in the curvature of $T_s(p)$. With increasing pressure, $T_s(p)$ changes from a concave to a convex curvature and shows a tendency to saturate before $T_s(p)$ is abruptly suppressed [see the phase diagram in Fig. 3(a)]. This behavior can be taken as a further indication of a first-order-like suppression of T_s. At low temperatures, we observe a strong variation of the normal state resistivity with pressure and zero resistance, indicating the development of a superconducting state [see Fig. 1(b)]. Applying pressure increases the superconducting transition temperature T_c. We note that the superconducting transition remains narrow at all pressures.

The residual resistivity ratio, equals to ρ_{300K}/ρ_{5K}, is the appropriate parameter to estimate the degree of disorder-related scattering present in a material. Figure 2(a) shows that the high-temperature resistivity ρ_{300K} decreases monotonically with pressure, but the RRR value is strongly suppressed in the mixed-phase region. The competition between the two

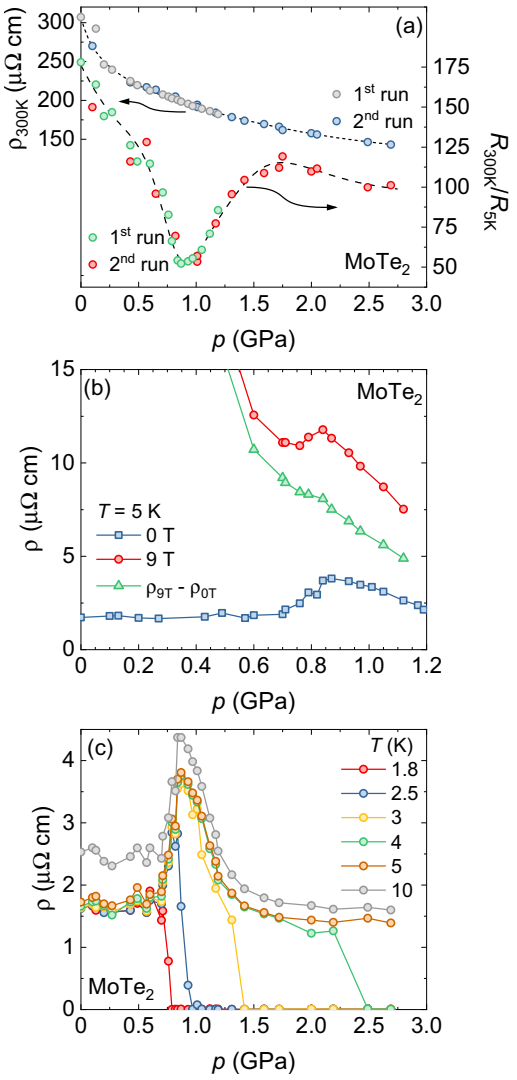

FIG. 2. (a). Left axis, electrical resistivity at 300 K (ρ_{300K}); right axis, RRR as a function of pressure. The dashed and dotted black lines are guides to the eyes. (b) $\rho(p)$ at 5 K at 0 and 9 T and the difference between the two curves. (c) Electrical resistivity (ρ) in the low-temperature range at selected temperatures as a function of pressure.

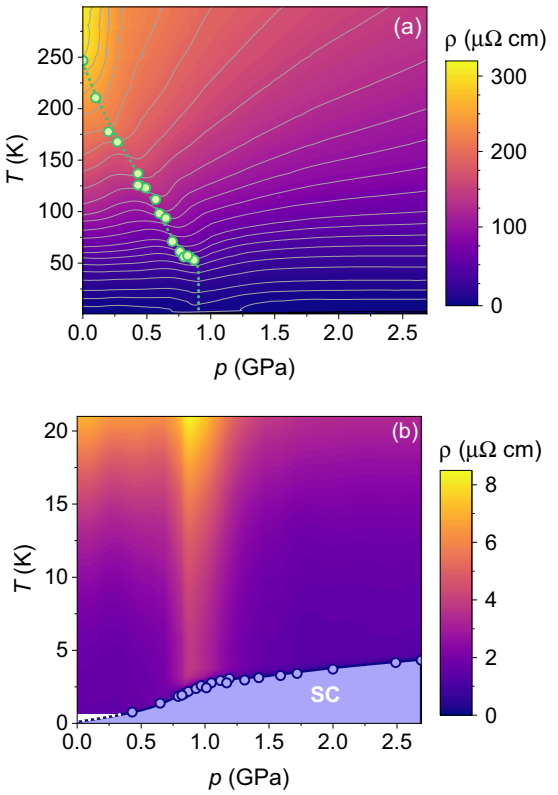

FIG. 3. (a, b) Color maps of the electrical resistivity (ρ) as a function of temperature for all studied pressures. Green and purple circles denote T_s and T_c, respectively. The gray lines in (a) are equipotential lines of the resistivity and the dotted lines are guides for the eye. The data used to create the color maps are shown in the Supplemental Material [39] and are available at Ref. [40].

structural phases leads to an enhancement of the structural disorder as well as the disorder-induced scattering in $MoTe_2$. The monotonic variation of $\rho_{300K}(p)$ precludes any extrinsic origin. A clear indication of the structural origin of the enhanced disorder in the mixed-phase region is obtained by subtracting the electrical resistivity at 0 T from the 9 T curve. As shown in Fig. 2(b), no resistivity anomaly is observed in the difference, ruling out a magnetic origin for the ρ enhancement. Remarkably, the superconducting state is not affected by the increasing disorder in the mixed-phase region, as T_c is monotonically enhanced with increasing pressure. Moreover, there is a sharp transition to the superconducting state that occurs independently of the pronounced changes in the resistivity value, as shown in Fig. 2(c).

In the following we reconcile the implications of the structural transition, i.e., an inversion symmetry breaking transition from the centrosymmetric $1T'$ to the noncentrosymmetric T_d phase, on the superconductivity, which has been proposed to be topological in the T_d phase. $\rho_{5K}(p)$, the isothermal resistivity at 5 K, is a good measure of the residual resistivity since there is little temperature variation in $\rho(T)$ at low temperatures $T \lesssim 10$ K and the sample is in the normal state at this temperature throughout the pressure window studied here [see Fig. 2(c)]. It is pressure independent with a value of 1.7 $\mu\Omega$ cm up to about 0.75 GPa, followed by a rapid rise to about 3.4 $\mu\Omega$ cm at 1.01 GPa. Upon further pressure increase, $\rho_{5K}(p)$ decreases again to a constant value of 1.4 $\mu\Omega$ cm, which is slightly smaller than the ambient pressure value. The pressure independent behavior in the low- and high-pressure region away from the mixed phase suggests that pressure does not lead to any kind of structural defects and only drives the structural phase transition from the T_d to the $1T'$ phase. The pronounced maximum in $\rho_{5K}(p)$ is therefore directly related to additional scattering contributions in the mixed-phase region and defines its range at low temperatures between about 0.75 and 1.4 GPa.

To better visualize the features present in the electrical resistivity of $MoTe_2$, we show a color map in Fig. 3(a). At high temperatures the structural transition (green symbols) produces a distinct feature in the resistivity equipotential lines. Below about 50 K the feature does not move with pressure and remains at about 0.8 GPa. This indicates the first-order-like suppression of T_s, which is convincingly shown in the

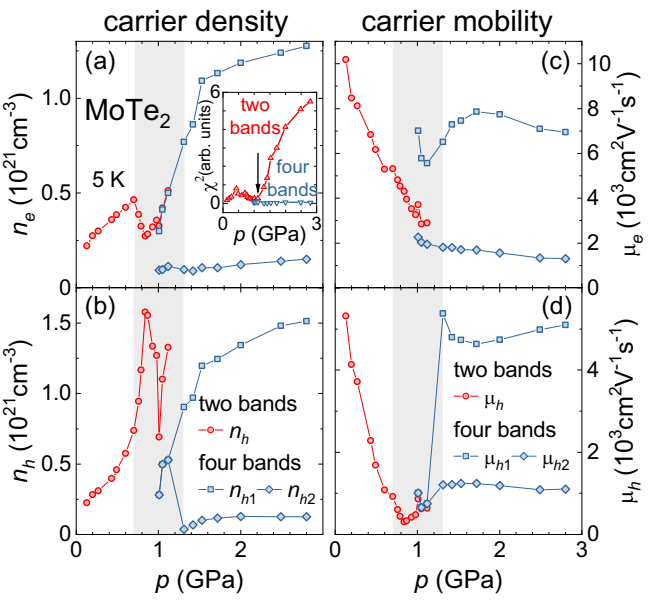

FIG. 4. Carrier densities for (a) electrons and (b) holes and mobilities for (c) electrons and (d) holes for $MoTe_2$. The inset in (a) presents the reduced χ^2 obtained with the fits considering two-band or four-band models. The highlighted area indicates that the coexistence region of the two structural phases T_d and $1T'$ occurs.

enlarged view of the low-temperature region in Fig. 3(b). The shading also indicates the region of increased structural disorder before the onset of superconductivity at lower temperatures. It is remarkable to see how the superconducting T_c increases smoothly in this region. This behavior is not expected for two separate superconducting phases with different order parameter symmetry in the $1T'$ and T_d structures and suggests the existence of a single superconducting phase in $MoTe_2$.

The analysis of the Hall conductivity gives more information about the carrier densities $n_{e(h)}$ and mobilities $\mu_{e(h)}$ (see the Supplemental Material [39] for further details). Here $e(h)$ denotes electronlike (holelike) charge carriers. We obtain the longitudinal $\sigma_{xx} = \rho_{xx}/(\rho_{xx}^2 + \rho_{xy}^2)$ and the transverse $\sigma_{xy} = -\rho_{xy}/(\rho_{xx}^2 + \rho_{xy}^2)$ conductivities from our electrical and Hall resistivities. In $MoTe_2$, the application of external pressure enhances the transport contribution of four pockets (two holes and two electrons), as previously reported [35]. Therefore, the two-band model is more suitable for pressures lower than 1.12 GPa, while a four-band model has been applied for higher pressures, as clearly evidenced by the reduced χ^2 obtained with the fits [see the inset of Fig. 4(a)]. In the mixed-phase region, the results of the two models partly overlap. Figure 4 summarizes the pressure evolution of the carrier densities and mobilities obtained from the transport data at 5 K for holes and electrons. At ambient pressure, the carrier density values are similar to previous reports [17]. The highlighted gray area represents the mixed-phase region. One can see a smooth increase in the carrier densities of both electrons and holes with increasing pressure, which then starts to decrease in the mixed-phase region, reaching a minimum at 0.84 GPa [see Figs. 4(a) and 4(b)]. Above this pressure the carrier densities start to increase again and saturate at high pressures for all four pockets. Both electron and hole mobilities are suppressed with increasing pressure and reach a minimum in the mixed-phase region [see Figs. 4(c) and 4(d)]. After the appearance of the new hole and electron pockets, the mobility for one pocket is almost pressure independent, while for the others it is strongly increased and then saturates above 1.5 GPa. These results highlight the distinct differences in the electronic properties of the $1T'$ and T_d phases, in contrast to the smooth evolution of the superconducting T_c as a function of pressure over the entire pressure range studied.

Our results show a smooth variation of $T_c(p)$, independent of the large increase in the residual resistivity, indicating enhanced disorder scattering, near the critical pressure where T_s is suppressed. Furthermore, pronounced changes in the electronic properties were evidenced by the distinct pressure evolution of the charge carrier density and mobility. These features enabled us to draw conclusions about the possible superconducting order parameter(s) in $MoTe_2$. A topological s^{+-} superconducting state has been proposed to be realized in the noncentrosymmetric T_d phase and a conventional s^{++} state in the centrosymmetric $1T'$ phase [27,41]. However, it is quite challenging to directly probe the relationship between the superconducting state and the crystalline structure as a function of pressure at temperatures below 5 K. While s^{++} superconductivity is nearly insensitive to structural disorder, s^{+-} is expected to be strongly suppressed by it [6,8]. We observe an enhancement of T_c with increasing pressure in the mixed-phase regime where the residual resistivity is maximal. This seems to rule out the possibility of topological s^{+-} pairing in $MoTe_2$. We therefore propose a scenario in which only the $1T'$ phase exhibits (conventional) superconductivity at low temperatures and the T_d phase remains normal at all pressures.

Previous studies proposing a topological s^{+-} pairing in $MoTe_2$ based on the suppression of T_c as a function of disorder did not consider the possible presence of the $1T'$ phase at low temperatures in the entire pressure range down to ambient pressure. Our proposal implies that a small amount of the $1T'$ phase is already present in the material at low pressures. Cho *et al.* actually report the presence of the $1T'$ phase at ambient pressure as a function of the residual resistivity ratio [42]. According to this work, the RRR equal to 178 of our sample would imply a very small fraction of the $1T'$ phase of a few percent present at ambient pressure. This is not inconsistent with other work claiming only the presence of the T_d phase at low temperatures, since such a small volume fraction of the $1T'$ phase may not be resolved in x-ray diffraction. Evidence for the presence of the $1T'$ phase at low pressures has been reported in Refs. [15,42] and no zero-resistance state has been observed in samples lacking the $1T'$ structure. We note that even a small volume fraction of the $1T'$ phase in the sample could cause a sharp superconducting jump in resistivity and produce a full-volume diamagnetic shielding in AC susceptibility experiments, as previously reported for polycrystalline samples [27]. The smooth evolution of $T_c(p)$ is also difficult to reconcile with an expected phase transition from a topological s^{+-} to a conventional s^{++} superconducting state. Our proposal of a (conventional) superconducting state in the $1T'$ phase, present over the entire pressure range at low temperatures, explains the observed behavior in a natural way.

In conclusion, we have performed a detailed investigation of the temperature-pressure phase diagram of $MoTe_2$ by electrical transport experiments. Our data reveal a first-order-like suppression of the structural phase transition and a strong increase of the disorder scattering contribution to the electrical resistivity in the mixed-phase regime around the first-order phase transition. Surprisingly, we find a smooth increase of the superconducting transition temperature over the whole pressure range. This leads us to conclude that topological s^{+-} superconductivity is most likely not realized in $MoTe_2$. Based on our data, we argue that only the $1T'$ phase exhibits superconductivity at low temperatures.

Data that underpin the findings of this Letter are available at Edmond—the open research data repository of the Max Planck Society [40].

We acknowledge fruitful discussions with M. Baenitz, T. Fuji, and H. Yasuoka. This project has received funding from the European Union's Horizon 2020 research and innovation program under Marie Skłodowska-Curie Grant No. 101019024. This work was also supported by São Paulo Research Foundation Grants No. 2018/0823-0, No. 2021/02314-9, and No. 2022/05447-2. Work at Brookhaven National Laboratory was supported by the U.S. Department of Energy, Office of Science, Office of Basic Energy Sciences under Contract No. DE-SC0012704 (materials synthesis). R.D.d.R. and L.O.K. acknowledge financial support from the Max Planck Society under the auspices of the Max Planck Partner Group R. D. dos Reis of the Max Planck Institute for Chemical Physics of Solids, Dresden, Germany.

[1] M. Y. He, H. M. Sun, and Q. L. He, Topological insulator: Spintronics and quantum computations, Front. Phys. **14**, 43401 (2019).

[2] M. M. Sharma, P. Sharma, N. K. Karn, and V. P. S. Awana, Comprehensive review on topological superconducting materials and interfaces, Supercond. Sci. Technol. **35**, 083003 (2022).

[3] C. Nayak, S. H. Simon, A. Stern, M. Freedman, and S. Das Sarma, Non-Abelian anyons and topological quantum computation, Rev. Mod. Phys. **80**, 1083 (2008).

[4] B. Lian, X. Q. Sun, A. Vaezi, X. L. Qi, and S. C. Zhang, Topological quantum computation based on chiral Majorana fermions, Proc. Natl. Acad. Sci. USA **115**, 10938 (2018).

[5] F. Wilczek, Majorana returns, Nat. Phys. **5**, 614 (2009).

[6] X.-L. Qi and S.-C. Zhang, Topological insulators and superconductors, Rev. Mod. Phys. **83**, 1057 (2011).

[7] M. Sato, Y. Takahashi, and S. Fujimoto, Non-Abelian topological orders and Majorana fermions in spin-singlet superconductors, Phys. Rev. B **82**, 134521 (2010).

[8] P. Hosur, X. Dai, Z. Fang, and X.-L. Qi, Time-reversal-invariant topological superconductivity in doped Weyl semimetals, Phys. Rev. B **90**, 045130 (2014).

[9] S. Paul, S. Talukdar, R. S. Singh, and S. Saha, Topological Phase Transition in $MoTe_2$: A Review, Phys. Status Solidi RRL **17**, 2200420 (2023).

[10] J. Guo and K. Liu, Recent progress in two-dimensional $MoTe_2$ hetero-phase homojunctions, Nanomater. **12**, 110 (2021).

[11] J. Cui, P. L. Li, J. D. Zhou, W. Y. He, X. W. Huang, J. Yi, J. Fan, Z. Q. Ji, X. N. Jing, F. M. Qu, Z. G. Cheng, C. L. Yang, L. Lu, K. Suenaga, J. W. Liu, K. T. Law, J. H. Lin, Z. Liu, and G. T. Liu, Transport evidence of asymmetric spin-orbit coupling in few-layer superconducting $1T_d - MoTe_2$, Nat. Commun. **10**, 2044 (2019).

[12] R. He, S. Zhong, H. H. Kim, G. Ye, Z. Ye, L. Winford, D. McHaffie, I. Rilak, F. Chen, X. Luo, Y. Sun, and A. W. Tsen, Dimensionality-driven orthorhombic $MoTe_2$ at room temperature, Phys. Rev. B **97**, 041410(R) (2018).

[13] H. Kowalczyk, J. Biscaras, N. Pistawala, L. Harnagea, S. Singh, and A. Shukla, Gate and temperature driven phase transitions in few-Layer $MoTe_2$, ACS Nano **17**, 6708 (2023).

[14] R. Clarke, E. Marseglia, and H. Hughes, A low-temperature structural phase transition in $\beta - MoTe_2$, Philos. Mag. B **38**, 121 (1978).

[15] C. Heikes, I. L. Liu, T. Metz, C. Eckberg, P. Neves, Y. Wu, L. D. Hung, P. Piccoli, H. B. Cao, J. Leao, J. Paglione, T. Yildirim, N. P. Butch, and W. Ratcliff, Mechanical control of crystal symmetry and superconductivity in Weyl semimetal $MoTe_2$, Phys. Rev. Mater. **2**, 074202 (2018).

[16] Y. P. Qi, P. G. Naumov, M. N. Ali, C. R. Rajamathi, W. Schnelle, O. Barkalov, M. Hanfland, S. C. Wu, C. Shekhar, Y. Sun, V. Suss, M. Schmidt, U. Schwarz, E. Pippel, P. Werner, R. Hillebrand, T. Forster, E. Kampert, S. Parkin, R. J. Cava *et al.*, Superconductivity in Weyl semimetal candidate $MoTe_2$, Nat. Commun. **7**, 11038 (2016).

[17] Y. J. Hu, Y. T. Chan, K. T. Lai, K. O. Ho, X. Y. Guo, H. P. Sun, K. Y. Yip, D. H. L. Ng, H. Z. Lu, and S. K. Goh, Angular dependence of the upper critical field in the high-pressure 1T' phase of $MoTe_2$, Phys. Rev. Mater. **3**, 034201 (2019).

[18] Y. J. Hu, W. C. Yu, K. T. Lai, D. Sun, F. F. Balakirev, W. Zhang, J. Y. Xie, K. Y. Yip, E. I. P. Aulestia, R. Jha, R. Higashinaka, T. D. Matsuda, Y. Yanase, Y. Aoki, and S. K. Goh, Detection of hole pockets in the candidate type-II Weyl semimetal $MoTe_2$ from Shubnikov-de Haas quantum oscillations, Phys. Rev. Lett. **124**, 076402 (2020).

[19] I. L. Liu, C. Heikes, T. Yildirim, C. Eckberg, T. Metz, H. Kim, S. Ran, W. D. Ratcliff, J. Paglione, and N. P. Butch, Quantum oscillations from networked topological interfaces in a Weyl semimetal, npj Quantum Mater. **5**, 62 (2020).

[20] H. Takahashi, T. Akiba, K. Imura, T. Shiino, K. Deguchi, N. K. Sato, H. Sakai, M. S. Bahramy, and S. Ishiwata, Anticorrelation between polar lattice instability and superconductivity in the Weyl semimetal candidate $MoTe_2$, Phys. Rev. B **95**, 100501(R) (2017).

[21] S. Dissanayake, C. R. Duan, J. J. Yang, J. Liu, M. Matsuda, C. M. Yue, J. A. Schneeloch, J. C. Y. Teo, and D. Louca, Electronic band tuning under pressure in $MoTe_2$ topological semimetal, npj Quantum Mater. **4**, 45 (2019).

[22] J. Yang, J. Colen, J. Liu, M. C. Nguyen, G.-w. Chern, and D. Louca, Elastic and electronic tuning of magnetoresistance in $MoTe_2$, Sci. Adv. **3**, eaao4949 (2017).

[23] M. G. Kanatzidis, Discovery-synthesis, design, and prediction of chalcogenide phases, Inorg. Chem. **56**, 3158 (2017).

[24] Z. Wang, D. Gresch, A. A. Soluyanov, W. Xie, S. Kushwaha, X. Dai, M. Troyer, R. J. Cava, and B. A. Bernevig, $MoTe_2$: A

type-II Weyl topological metal, Phys. Rev. Lett. **117**, 056805 (2016).

[25] D. Rhodes, R. Schönemann, N. Aryal, Q. Zhou, Q. R. Zhang, E. Kampert, Y.-C. Chiu, Y. Lai, Y. Shimura, G. T. McCandless, J. Y. Chan, D. W. Paley, J. Lee, A. D. Finke, J. P. C. Ruff, S. Das, E. Manousakis, and L. Balicas, Bulk Fermi surface of the Weyl type-II semimetallic candidate $\gamma - MoTe_2$, Phys. Rev. B **96**, 165134 (2017).

[26] X. Luo, F. C. Chen, J. L. Zhang, Q. L. Pei, G. T. Lin, W. J. Lu, Y. Y. Han, C. Y. Xi, W. H. Song, and Y. P. Sun, T-d-$MoTe_2$: A possible topological superconductor, Appl. Phys. Lett. **109**, 136 (2016).

[27] Z. Guguchia, F. von Rohr, Z. Shermadini, A. T. Lee, S. Banerjee, A. Wieteska, C. Marianetti, B. Frandsen, H. Luetkens, Z. Gong *et al.*, Signatures of the topological s^{+-} superconducting order parameter in the type-II Weyl semimetal $T_d - MoTe_2$, Nat. Commun. **8**, 1082 (2017).

[28] J. W. Luo, Y. N. Li, J. W. Zhang, H. R. Ji, H. Wang, J. Y. Shan, C. X. Zhang, C. Cai, J. Liu, Y. Wang, Y. Zhang, and J. Wang, Possible unconventional two-band superconductivity in $MoTe_2$, Phys. Rev. B **102**, 064502 (2020).

[29] A. Jindal, A. Saha, Z. Li, T. Taniguchi, K. Watanabe, J. C. Hone, T. Birol, R. M. Fernandes, C. R. Dean, A. N. Pasupathy *et al.*, Coupled ferroelectricity and superconductivity in bilayer Td-$MoTe_2$, Nature (London) **613**, 48 (2023).

[30] R. M. Fernandes, A. I. Coldea, H. Ding, I. R. Fisher, P. Hirschfeld, and G. Kotliar, Iron pnictides and chalcogenides: a new paradigm for superconductivity, Nature (London) **601**, 35 (2022).

[31] P. Szabó, P. Samuely, J. Kačmarčík, T. Klein, J. Marcus, D. Fruchart, S. Miraglia, C. Marcenat, and A. G. M. Jansen, Evidence for two superconducting energy gaps in MgB_2 by point-contact spectroscopy, Phys. Rev. Lett. **87**, 137005 (2001).

[32] Y. Li, Q. Gu, C. Chen, J. Zhang, Q. Liu, X. Hu, J. Liu, Y. Liu, L. Ling, M. Tian *et al.*, Nontrivial superconductivity in topological $MoTe_{2-x}S_x$ crystals, Proc. Natl. Acad. Sci. USA **115**, 9503 (2018).

[33] F. Chen, X. Luo, R. Xiao, W. Lu, B. Zhang, H. Yang, J. Li, Q. Pei, D. Shao, R. Zhang *et al.*, Superconductivity enhancement in the S-doped Weyl semimetal candidate $MoTe_2$, Appl. Phys. Lett. **108**, 162601 (2016).

[34] Y. Zhang, F. Fei, R. Liu, T. Zhu, B. Chen, T. Qiu, Z. Zuo, J. Guo, W. Tang, L. Zhou *et al.*, Enhanced superconductivity and upper critical field in Ta-doped Weyl semimetal $T_d - MoTe_2$, Adv. Mater. **35**, 2207841 (2023)..

[35] S. Lee, J. Jang, S.-I. Kim, S.-G. Jung, J. Kim, S. Cho, S. W. Kim, J. Y. Rhee, K.-S. Park, and T. Park, Origin of extremely large magnetoresistance in the candidate type-II Weyl semimetal $MoTe_{2-x}$, Sci. Rep. **8**, 1 (2018).

[36] G. Ghigo, D. Torsello, G. A. Ummarino, L. Gozzelino, M. A. Tanatar, R. Prozorov, and P. C. Canfield, Disorder-driven transition from $s_{\pm}$ to s_{++} superconducting order parameter in proton irradiated $Ba(Fe_{1-x}Rh_x)_2As_2$ single crystals, Phys. Rev. Lett. **121**, 107001 (2018).

[37] M. Nicklas, Pressure probes, in *Strongly Correlated Systems* (Springer, New York, 2015), pp. 173–204.

[38] H. Takahashi, K. Hasegawa, T. Akiba, H. Sakai, M. S. Bahramy, and S. Ishiwata, Giant enhancement of cryogenic thermopower by polar structural instability in the pressurized semimetal $MoTe_2$, Phys. Rev. B **100**, 195130 (2019).

[39] See Supplemental Material at http://link.aps.org/supplemental/10.1103/PhysRevMaterials.7.L111801 for additional information on the two-band and four-band model fits of the longitudinal and Hall conductivity. It also contains the electrical resistivity as a function of temperature at every studied pressure. It includes Ref. [35].

[40] See M. Moda Piva, Data for the manuscript entitled "Superconducting pairing symmetry in MoTe2," in Edmond, https://doi.org/10.17617/3.WSL8ZP.

[41] Z. Guguchia, A. M. dos Santos, F. O. von Rohr, J. J. Molaison, S. Banerjee, D. Rhodes, J. X. Yin, R. Khasanov, J. Hone, Y. J. Uemura, M. Z. Hasan, H. Luetkens, E. S. Bozin, and A. Amato, Pressure induced topological quantum phase transition in Weyl semimetal $T_d - MoTe_2$, J. Phys. Soc. Jpn. **89**, 094707 (2020).

[42] S. Cho, S. H. Kang, H. S. Yu, H. W. Kim, W. Ko, S. W. Hwang, W. H. Han, D. H. Choe, Y. H. Jung, K. J. Chang, Y. H. Lee, H. Yang, and S. W. Kim, Te vacancy-driven superconductivity in orthorhombic molybdenum ditelluride, 2D Mater. **4**, 021030 (2017).